Drug & Virus Transport across Biological Barriers: Interactions, Diffusion, Partitioning, Permeability, and Selectivity

Mikael O. Ellingson and Michael A. Bevan†
Chemical & Biomolecular Engr., Johns Hopkins Univ., Baltimore, MD 21218

Table of Contents

List of Supplemental Figures

Theory

Sphere-Pore Hydrodynamics

For a position-averaged diffusivity, the hydrodynamic resistance at every location within a pore must be known. First, a particle with a hard-core and a partially permeable layer has an effective hydrodynamic radius expressed as (**Fig. S1A**),[1]

$$a_H = a + [1-\phi]L \tag{S1}$$

where a is the hard-core radius, a_H is the hydrodynamic radius, ϕ is polymer layer solvent-permeability, and L is the total thickness of the layer – where the polymer density goes to zero. In practice, ϕ depends theoretically on the polymer density profile and the hydrodynamic (Brinkman) permeability of the polymer solution, but could be measured, as in our recent prior work.[1] There are no exact analytical models of the sphere-cylindrical pore hydrodynamic friction. Thus, approximations must be made, interpolating between available limiting cases. Axial motion along the centerline of a cylinder with no-slip and impermeable boundary conditions has been computationally found, and analytically expressed.[2] However, no other result generalizes this form to arbitrary position in the pores.[3-4] A rational expression can be used to express the centerline hydrodynamics as,

$$f_{\|,c}(a_H, R) = \frac{2(a_H/R)^3 - 3(a_H/R)^2 - 2(a_H/R) + 3}{65(a_H/R)^3 - 17(a_H/R)^2 + 6(a_H/R) + 3} \tag{S2}$$

The coefficients were derived by fitting a digitized version of exact theory curve of centerline-

†To whom correspondence should be addressed. email: mabevan@jhu.edu

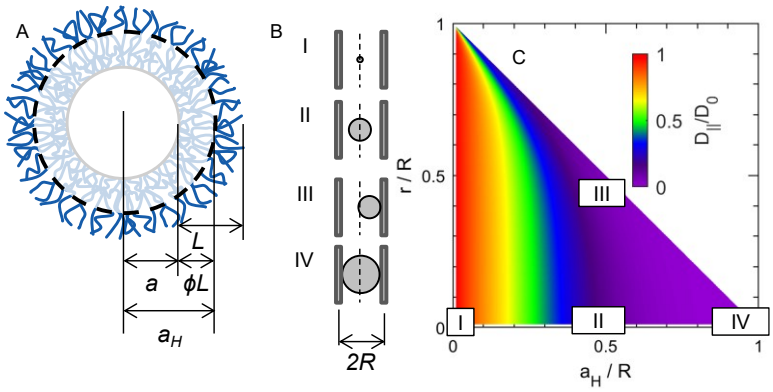

Fig. S1. **Approximating sphere-in-pore hydrodynamic interactions.** (A) Diagram explaining the difference between the hard-core radius, a, and the hydrodynamic radius, a_H, due to a brush layer, L, with partial solvent permeability, ϕ. (B) Diagram showing four different limiting cases. I, small particles on centerline; II, moderate particles on centerline; III, moderate particles approaching pore wall; and IV, particle size approaching pore size. (C) Hydrodynamic mobility coefficient (Eq. (S3)) as a function of both particle size and particle position, with callouts for the four limiting cases of B.

pore hydrodynamic.[2] For the simplest form, consider the linear interpolation between centerline (Eq. (S2)) and particle-wall contact value,[5] which matches the linear asymptote for the lubrication limit,

$$D_{||}(r,a_H,R) = D_0 H_{||,c}(r,a_H,R) = D_0\left[\left(f_{||,c}(a_H,R) - f_{||,w}\right)(R-a_H-r)/(R-a_H) + f_{||,w}\right] \quad \text{(S3)}$$

Note that this form hits the limits for (e.g. **Fig. S1B**): (1) small particles, which have Stokes-Einstein diffusivity in the limit; (2) moderate particles at centerline, which always gives the centerline result; (3) moderate particles at pore contact, which follows the lubrication theory limiting contact value ($f_{||,w} \approx 0.32$);[5] and (4) pore-sized particles, which tends to a diffusivity of zero, consistent with the lubrication limit of nearly pore-sized particles.[5] This allows for the prediction of hydrodynamics at any particle-pore-position **Fig. S1C**. Further development of this theory could be done by comparisons to numerical simulations or direct experiments of the particle-pore hydrodynamics. It is unlikely that an analytical solution for the full hydrodynamic equation is forthcoming, given the lack of progress since original, partially complete predictions.[2] Explicit fiber matrices would have less friction due to the longer range motion of solvent. To better capture the hydrodynamic friction in this cylinder model, solving the centerline mobility could be done with a partially permeable wall boundary condition. This could potentially be approximated by increasing the centerline and particle-wall contact mobilities closer to 1.

Derjaguin Approximation for Spheres within Cylindrical Pores

The Derjaguin approximation allows for the use of planar potentials (between half spaces) to model the interaction between arbitrarily curved surfaces, parametrized by the product of the principle curvatures at nearest approach,[6-8]

$$U(r) = 2\pi\left(\lambda_1\lambda_2\right)^{-1/2}\int_{R-a-r}^{\infty}\Delta G(\delta)d\delta \quad \text{(S4)}$$

where λ_1, λ_2 are the principal curvatures of the two surfaces at the distance of closest approach, and ΔG is the free energy per unit area of the surface-medium-surface system at a given separation, L. For spherical particles in pores, the product of the principal curvatures are,[9]

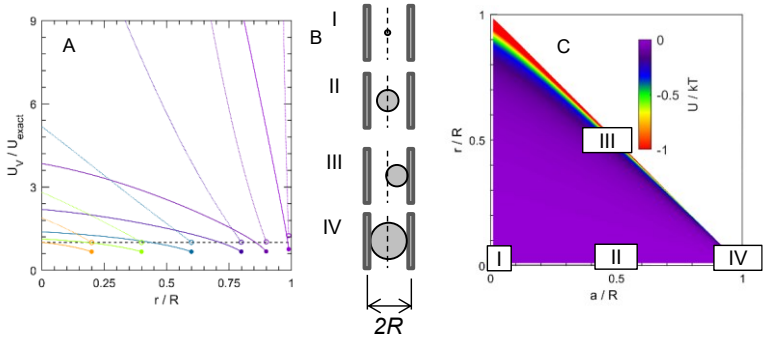

Fig. S2. **Developing sphere-in-pore interaction potentials.** (A) Development of the improved approximation to the van Der Waals interactions potential, correcting just Derjaguin (Eq. (S9), dashed lines), to the final form (Eq. (S10), solid line). (B) Diagram showing four different limiting cases. I, small particles on centerline; II, moderate particles on centerline; III, moderate particles approaching pore wall; and IV, particle size approaching pore size. (C) Comparison of exact Van Der Waals interaction near walls potentials and improved form, incorporating Derjaguin approximation and additional position correction (Eq. (S10)), with callouts for the four limiting cases of B.

$$(\lambda_1\lambda_2)^{-1/2} = a\left(1-a/R\right)^{-1/2}$$
$$U(r) = 2\pi a\left(1-a/R\right)^{-1/2}\int_{R-a-r}^{\infty}\Delta G(\delta)d\delta \tag{S5}$$

For polymer brushes on planar surfaces, the free energy of compression can be given by an exponential form as,[10]

$$\Delta G(h) = 57.9 f_0 \exp(-20.8\,h/2L) \tag{S6}$$

where L is the steric length of the polymer layer, and f_0 is the uncompressed brush free energy per unit area. Using Eq.(S4), the particle-pore interaction from brush interactions becomes,

$$U_S(r) = \Gamma a\left(1-a/R\right)^{-1/2}\exp\left(-\gamma\left[R-a-r\right]\right) \tag{S7}$$

where $\Gamma=115.8\pi f_0$, and $\gamma=5.2/L$.[10] The van der Waals interaction exists between any two materials, dependent on the material properties. The potential energy of interaction between two planar surfaces at the short range can be found be the Hamaker integration,

$$\Delta G(\delta) = -A/12\pi\delta^2 \tag{S8}$$

Using Eq.(S4) to convert the planar geometry to that of sphere-pore, the particle-pore interaction from van der Waals interactions becomes,

$$U_V(r) = -Aa/6\left(1-a/R\right)^{-1/2}\left(R-a-r\right)^{-1} \tag{S9}$$

Eq. (S9) yields a reasonable approximation to the van der Waals interaction potential for spheres-in-pores (**Fig. S2A**). However, numerical and limiting analytical expressions exists to the sphere-in-pore Hamaker integration.[9, 11] Comparing the inner analytical solution to a range of particle-pore size ratios allows for an additional correction factor to be applied, bringing this simple analytic expression to higher accuracy throughout the position, particle size, and pore size space (**Fig. S2B**), as,

$$U_V(r) = Aa/66\left(R/a - r/a\right)^{-1}\left(1 - a/R\right)^{-1/2}\left(R - a - r\right)^{-1} \tag{S10}$$

which is plotted in **Fig. S2C**.

Partitioning of Spherical Particles into Cylindrical Pores

The partitioning of a particle or macromolecule in a cylindrical pore can be described by,[12]

$$K = \frac{\int_0^{2\pi}\int_0^{L}\int_0^{R} \exp\left(-U(r)/kT\right) r\,dr\,dz\,d\theta}{\lim_{a\to 0}\int_0^{2\pi}\int_0^{L}\int_0^{R} \exp\left(-U_H(r)/kT\right) r\,dr\,dz\,d\theta} \tag{S11}$$

where r,z,θ are the radial, axial and angular coordinates of a pore-axis aligned cylindrical coordinate systems. For spheres-in pores, axisymmetric geometry, radial symmetry, and no axial dependence assumptions allow the form to the simplified to,

$$K = \frac{2}{R^2}\int_0^{R} \exp\left(-U(r)/kT\right) r\,dr \tag{S12}$$

Consider that these potentials have hard-wall and colloidal (or long-range) interactions, U(r) = $U_H(r)$ + $U_C(r)$. Without the colloidal potential, there are only hard-wall effects, leaving purely entropic contributions to the partitioning.[12-15] The piece-wise integration of the hard-wall potential,

$$\begin{aligned} K_{HS} &= \frac{2}{R^2}\int_0^{R} \exp\left(-\left[\cancel{U_C(r)} + U_H(r)\right]/kT\right) r\,dr \\ &= \frac{2}{R^2}\left[\int_0^{R-a} \exp\left(-0/kT\right) r\,dr + \int_{R-a}^{R} \exp\left(-\infty/kT\right) r\,dr\right] \\ &= \left(1 - a/R\right)^2 \end{aligned} \tag{S13}$$

The infinite energy case leads to an integrand of zero in the second term, whereas the first term has an integrand of identically *r*, allowing for the analytical expression for partitioning. This function is plotted in **Fig. 3B,C**. Size-exclusion effects means that the partitioning is always below one for hard-particles. Further, the partitioning tends towards zero as the particle approaches the pore size. By now considering the full potentials, U(r) = $U_H(r)$ + $U_C(r)$, it follows that,

$$\begin{aligned} K &= \frac{2}{R^2}\int_0^{R} \exp\left(-\left[U_C(r) + U_H(r)\right]/kT\right) r\,dr \\ &= \frac{2}{R^2}\int_0^{R-a} \left[\exp\left(-U_C(r)/kT\right) - 1\right] r\,dr + \left(1 - a/R\right)^2 \end{aligned} \tag{S14}$$

Transient and Steady State Flux through Barrier Films

Fick's first law describes the diffusive motion down a concentration gradient as,

$$j = -D\,\partial\rho C/\partial z \tag{S15}$$

The transient version of this partial differential equation has been solved in a variety of geometries

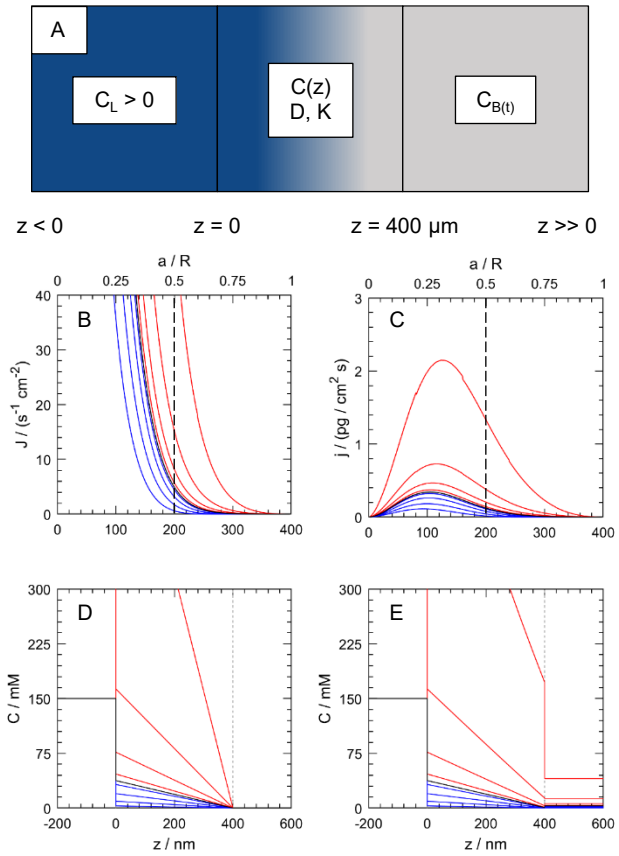

Fig. S3. Barrier film models for steady state and transient transport. (A) different compartments; left, lung-lumen; middle, mucus barrier; and, right, epithelium/blood. (B-E) Plots of the transport characteristics of particles with exponential interactions U(r) = B exp(-κ(R-a-r)). With B = -6-1000 kT. Attractive potentials (B < 0, red), no hard-wall interactions only (B = 0, black), and repulsive potentials (B > 0, blue) (B-C) flux through the barrier based on the (B) number of particles or (C) mass of particles. (D-E) Concentration profiles for 200-nanometer particles (vertical line in (B-C)) for (D) steady state model (Eq. (S21)) and (E) transient model (Eq. (S19))

and initial conditions, assisting the measurements of transport properties by time-lag analyses.[16] Specifically, the transient mass flux from a semi-infinite reservoir to a finite reservoir through a permeable membrane (**Fig. S3A**) with partitioning can be calculated by,[17]

$$j(t) = KD\rho C_\infty f(t)/l \tag{S16}$$

where $f(t)$ is a dimensionless factor,

$$f(t) = \sum_{n=1}^{\infty} 2\frac{(H^2+Q_n^2)\cos(Q_n)}{(H+H^2+Q_n^2)}\exp(-Q_n^2 t/[l^2/D]) \tag{S17}$$

where Q_n is the nth non-zero root of Q tan Q = H, and H is the scaled membrane to reservoir volume ratio, KV_m/V_R. This is plotted in **Fig. S3B**, with the corresponding mass flux curves in **Fig. S3C**. Flux expressions are proportional to the product of partitioning (K) and diffusivity (D), indicating that their combination, the permeability is a natural measure to optimize,

$$P = KD \tag{S18}$$

This is the flux expression resulting from the predicted concentration profile,

$$C(z,t) = C_0[1 - g(z,t)]$$
$$g(z,t) = 2\sum_{n=1}^{\infty} \frac{(H^2 + Q_n^2)}{(H + H^2 + Q_n^2)Q_n} \sin(Q_n z/l) \exp(-DQ_n^2 t/l^2) \quad \text{(S19)}$$

Additionally, the steady state solution for a similar problem – namely the transfer from semi-infinite to empty semi-infinite reservoir – has a very similar form,

$$j_{SS} = KD\rho C_\infty / l \quad \text{(S20)}$$

The only difference is the infinite sum multiplicative factor. From 1-15 minutes, typical for mucus clearance,[18] the transient (Eq. (S16)) and steady state (Eq. (S20)) expressions have less than 5% deviations for the hard-wall models shown in **Fig. S3**. Thus, the steady state flux is a reasonable model for the flux in moderate times, with additional accuracy available through the use of the full transient model. This flux is derived from the steady state concentration profile,

$$C = C_0[1 - z/l] \quad \text{(S21)}$$

References

1. Ellingson, M. O.; Bevan, M. A. Direct Measurements & Simplified Models of Colloidal Interactions & Diffusion with Adsorbed Macromolecules. *Soft Matter* **2024,** *20*, 6808-6821.
2. Happel, J.; Brenner, H. *Low Reynolds Number Hydrodynamics: With Special Applications to Particulate Media*. Martinus Nijhoff Publishers: Boston, **1983**.
3. Mavrovouniotis, G. M.; Brenner, H. Hindered Sedimentation, Diffusion, and Dispersion Coefficients for Brownian Spheres in Circular Cylindrical Pores. *Journal of Colloid and Interface Science* **1988,** *124*, 269-283.
4. Deen, W. M. Hindered Transport of Large Molecules in Liquid-Filled Pores. *AIChE Journal* **1987,** *33*, 1409-1425.
5. Pawar, Y.; Anderson, J. L. Hindered Diffusion in Slit Pores: An Analytical Result. *Industrial & Engineering Chemistry Research* **1993,** *32*, 743-746.
6. White, L. R. On the Deryaguin Approximation for the Interaction of Macrobodies. *Journal of Colloid and Interface Science* **1983,** *95*, 286-288.
7. Derjaguin, B. Untersuchungen Über Die Reibung Und Adhäsion, Iv. *Kolloid-Zeitschrift* **1934,** *69*, 155-164.
8. Torres-Díaz, I.; Bevan, M. A. General Potential for Anisotropic Colloid−Surface Interactions. *Langmuir* **2017,** *33*, 4356−4365.
9. Bhattacharjee, S.; Sharma, A. Apolar, Polar, and Electrostatic Interactions of Spherical Particles in Cylindrical Pores. *Journal of Colloid and Interface Science* **1997,** *187*, 83-95.
10. Ellingson, M. O.; Bevan, M. A. Kt- & Fn- Scale Polymer Brush Interactions: Theory Vs. Experiment for Aqueous Polyethylene Glycol Layers. *Macromolecules* **2025,** *58*, 9044-9054.
11. Bhattacharjee, S.; Sharma, A. Lifshitz-Van Der Waals Energy of Spherical Particles in Cylindrical Pores. *Journal of Colloid and Interface Science* **1995,** *171*, 288-296.
12. Giddings, J. C.; Kucera, E.; Russell, C. P.; Myers, M. N. Statistical Theory for the Equilibrium Distribution of Rigid Molecules in Inert Porous Networks. Exclusion Chromatography. *The Journal of Physical Chemistry* **1968,** *72*, 4397-4408.
13. Laurent, T. C.; Killander, J. A Theory of Gel Filtration and Its Experimental Verification. *Journal of Chromatography A* **1964,** *14*, 317-330.
14. Ogston, A. G. The Spaces in a Uniform Random Suspension of Fibres. *Transactions of the Faraday Society* **1958,** *54*, 1754-1757.
15. Ogston, A. G.; Phelps, C. F. The Partition of Solutes between Buffer Solutions and Solutions Containing Hyaluronic Acid. *Biochemical Journal* **1961,** *78*, 827-833.

16. Petropoulos, J. H. Membranes with Non-Homogeneous Sorption and Transport Properties. *Advances in Polymer Science* **1985,** *64*, 93-142.
17. Barrie, J. A.; Spencer, H. G.; Quig, A. Transient Diffusion through a Membrane Separating Finite and Semi-Infinite Volumes. *Journal of the Chemical Society, Faraday Transactions 1: Physical Chemistry in Condensed Phases* **1975,** *71*, 2459-2467.
18. Duncan, G. A.; Jung, J.; Hanes, J.; Suk, J. S. The Mucus Barrier to Inhaled Gene Therapy. *Molecular Therapy* **2016,** *24*, 2043-2053.